

## Hydrogen Bonding: A Channel for Protons to Transfer through Acid–Base Pairs

Liang Wu,<sup>†,‡</sup> Chuanhui Huang,<sup>†</sup> Jung-Je Woo,<sup>‡</sup> Dan Wu,<sup>†,‡</sup> Sung-Hyun Yun,<sup>‡</sup> Seok-Jun Seo,<sup>‡</sup> Tongwen Xu,<sup>\*,†</sup> and Seung-Hyeon Moon<sup>\*,‡</sup>

*Laboratory of Functional Membranes, School of Chemistry and Materials Science, University of Science and Technology of China, Hefei, Anhui 230026, People's Republic of China, and Department of Environmental Science and Engineering, Gwangju Institute of Science and Technology, Gwangju, 500-712 Republic of Korea*

Received: June 19, 2009; Revised Manuscript Received: July 31, 2009

Different from  $\text{H}_3\text{O}^+$  transport as in the vehicle mechanism, protons find another channel to transfer through the poorly hydrophilic interlayers in a hydrated multiphase membrane. This membrane was prepared from poly(phthalazinone ether sulfone ketone) (SPPESK) and  $\text{H}^+$ -form perfluorosulfonic resin (FSP), and poorly hydrophilic electrostatically interacted acid–base pairs constitute the interlayer between two hydrophilic phases (FSP and SPPESK). By hydrogen bonds forming and breaking between acid–base pairs and water molecules, protons transport directly through these poorly hydrophilic zones. The multiphase membrane, due to this unique transfer mechanism, exhibits better electrochemical performances during fuel cell tests than those of pure FSP and Nafion-112 membranes: 0.09–0.12  $\text{S cm}^{-1}$  of proton conductivity at 25 °C and 990  $\text{mW cm}^{-2}$  of the maximum power density at a current density of 2600  $\text{mA cm}^{-2}$  and a cell voltage of 0.38 V.

### Introduction

As an important subject of solution chemistry,<sup>1,2</sup> the study on proton transfer in homogeneous media, i.e., bulk water, was started by Eigen and De Maeyer.<sup>3,4</sup> They proposed two hydrogen-bonded frameworks for hydrated proton species in aqueous solutions: the Zundel cation  $\text{H}_5\text{O}_2^+$  and the Eigen cation  $\text{H}_9\text{O}_4^+$ . Intermolecular proton transfer occurs in these hydrogen-bonded frameworks, and its mechanism is the transformation between these two cations by hydrogen bonds breaking and forming (termed “structure diffusion”).<sup>3</sup> On the other hand, the diffusion of protonated water molecules ( $\text{H}_3\text{O}^+$ ) may make a certain contribution to the total proton conductivity (the vehicle mechanism<sup>5</sup>) for the high self-diffusion coefficient of water molecules. However, the diffusion of  $\text{H}_3\text{O}^+$  may be retarded in bulk water by the strong hydrogen bonding between water and the cations.<sup>6</sup>

Compared to the structure diffusion mentioned above, proton transfer in hydrated functionalized polymers (promising for application in proton exchange membrane fuel cells (PEMFCs)<sup>7</sup>) is much more complex due to the typical nanoseparation inside hydrated polymers. Such polymers combine in one macromolecule the hydrophilic character of terminal acidic functional groups (usually  $-\text{SO}_3\text{H}$ ) and the hydrophobic of the polymer backbone (perfluorinated or aromatic high-performance polymers).<sup>8</sup> In the presence of water, there occurs hydrophilic/hydrophobic separation: the acidic functional groups usually condense into a well-connected hydrophilic domain which facilitates proton conduction. At a very high water content (higher than 14  $\text{H}_2\text{O}$  per  $-\text{SO}_3\text{H}$ ), proton mobility is larger than the water self-diffusion coefficient, and the major mechanism of proton conduction is structure diffusion.<sup>9</sup> As water content decreases (13~6  $\text{H}_2\text{O}$  per  $-\text{SO}_3\text{H}$ ), however, proton mobility is close to or even lower than water self-diffusion, and the proton mobility in moderate hydration degree is essentially vehicular

in nature.<sup>10,11</sup> At a very low water content (lower than 6  $\text{H}_2\text{O}$  per  $-\text{SO}_3\text{H}$ ), the strong association of protonic charge carriers ( $-\text{SO}_3^-$ ) and counterions ( $\text{H}_3\text{O}^+$ ) makes it difficult to transfer in the vehicle mechanism.<sup>8</sup> The superior transport property of the Nafion membrane, which is widely used in fuel cells, is usually considered to follow the vehicle mechanism; however, proton transport is sometimes accompanied by parasitic transport (such as water permeability). Consequently, membranes with high proton conductivity at low water content are highly desirable since this would make water permeability less critical. Meanwhile, studies on proton transfer under such circumstances are of significance.

In this research, we present a new insight of the proton transfer in multiphase membranes, in which phase domains have different water contents. The membrane was prepared from a blend of  $\text{Na}^+$ -form sulfonated poly(phthalazinone ether sulfone ketone) (SPPESK) and  $\text{H}^+$ -form perfluorosulfonic resin (FSP). The chemical structures of these two polymers are shown in Figure 3a,b. This acid–base composite membrane is chosen for conventional characterizations and fuel cell tests, and the results will give information on the special proton transport through a poorly hydrophilic self-assembled phase.

### Experimental Section

**Materials.** FSP resins (IEC = 0.91 mmol g<sup>-1</sup>) were kindly supplied from Shandong Dongyue Polymer Materials (Zibo, China). SPPESK with a sulfonation degree of 114% was synthesized by following a procedure as previously reported.<sup>12</sup> Both of the polymers were transformed to the  $\text{Na}^+$  form by soaking them in 1 M NaOH for 24 h. *N,N'*-Dimethylformamide (DMF) was of reagent grade and used as received. Deionized water was obtained by circulating distilled water through a milli-Q water purification system. All other reagents and chemicals were of analytical grade and were used without further purification.

**Procedure for Preparation of the FSP/SPPESK Composite Membrane.** A 25 wt %  $\text{Na}^+$ -form FSP/DMF solution was obtained by dissolving FSP resins in DMF in an autoclave at

\* Corresponding author. E-mail: twxu@ustc.edu.cn; shmoon@gist.ac.kr.

† University of Science and Technology of China.

‡ Gwangju Institute of Science and Technology.

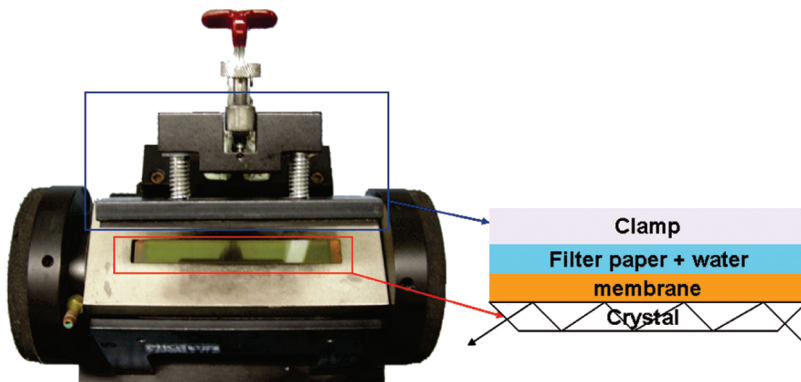


**Figure 1.** Schematic of ATR cell equipped with a clamp.

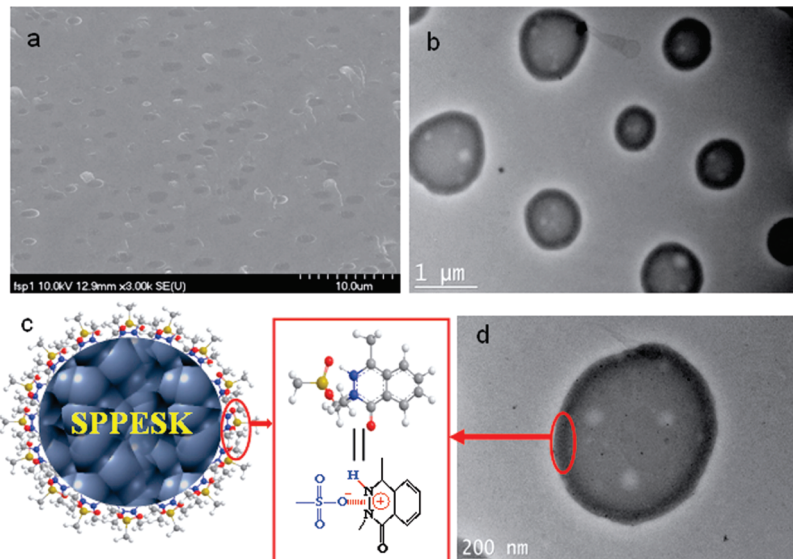


**Figure 2.** (a) SEM image of the cross-section of a (100%HFSP)-85 membrane> (b) and (d) TEM images with different magnification were obtained from a solution of (100% HFSP)-85 blend in DMF. (c) Possible SPPESK-encapsulated structure.

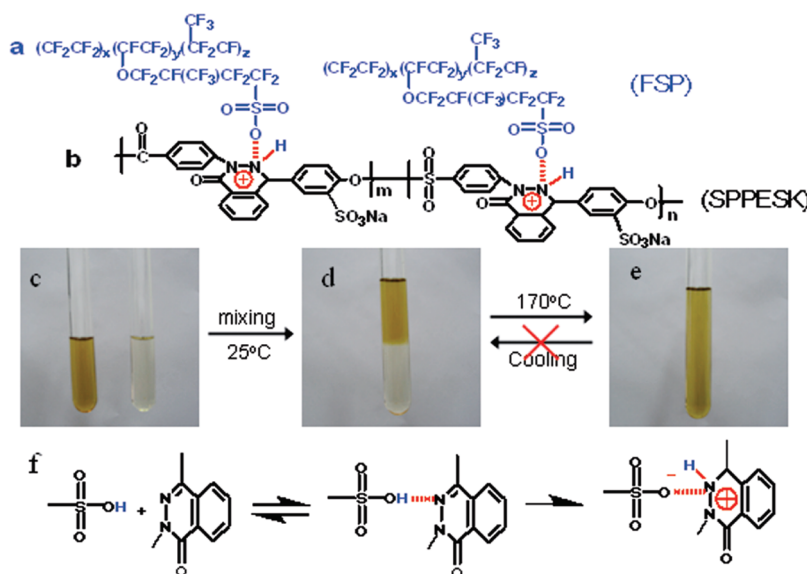


**Figure 3.** Chemical structure of FSP(a)/SPPESK(b) acid–base composite membrane. DMF solutions of SPPESK and FSP (c), FSP/SPPESK mixture (d), and FSP/SPPESK blend (e). Chemical reactions are shown in (f).

160 °C for 5 h. After purification by centrifugation, the solution was cast on a clean glass plate and dried at 100 °C for 24 h to remove solvent. Then, the FSP membrane with a thickness of approximately 60  $\mu\text{m}$  was obtained. Next, to prepare the FSP film with a controlled protonation degree, a salt/acid uptake

experiment was designed to determine the FSP partitioning equilibrium in external HCl/NaCl mixture solutions.<sup>13</sup> The dry membranes were equilibrated in an aqueous NaCl/HCl mixture solution with a preset  $\text{Na}^+/\text{H}^+$  concentration ratio. There was partial exchange of protons with  $\text{Na}^+$  on the FSP ion-exchange

sites, establishing the protonation degree of the FSP membrane. The FSP membranes with controlled protonation degrees were first washed with deionized water (all of the  $\text{Cl}^-$  ions were removed from the membranes), and the protonation degree of FSP could be calculated using the following equation

$$\text{protonation degree (\%)} = 100 \text{IEC}_{\text{Na}/\text{H}} / \text{IEC}_{100\% \text{H}} \quad (1)$$

where  $\text{IEC}_{\text{Na}/\text{H}}$  represented the IEC value of the partially protonated FSP, while  $\text{IEC}_{100\% \text{H}}$  represented the IEC value of the fully protonated FSP ( $0.91 \text{ mmol g}^{-1}$ ). Furthermore, those FSP membranes with different protonation degrees were dried and mixed with an appropriate amount of  $\text{Na}^+$ -formed SPPESK in DMF using an autoclave at  $160^\circ\text{C}$  for 5 h. The solution was cast onto a glass plate and dried at  $80^\circ\text{C}$  for 2 h and at  $120^\circ\text{C}$  for another 10 h to evaporate the solvent completely. The final membranes were cooled slowly in an oven (about  $9^\circ\text{C/min}$ ). The resulting membranes ( $50\text{--}70 \mu\text{m}$  in wet thickness) were removed from the glass plate and heated in boiling deionized water to remove impurities. The final membranes were donated as  $(x\% \text{HFSP})\text{-y}$ , in which  $x$  and  $y$  represented the protonation degree of FSP and FSP component weight content, respectively. These membranes were stored in water at room temperature for later use.

**Ion Exchange Capacity (IEC).** IEC was determined by using the Mohr method. The membrane in the  $\text{H}^+$  form was converted to the  $\text{Na}^+$  form after immersing in a  $\text{NaCl}$  aqueous solution ( $0.5 \text{ mol dm}^{-3}$ ) for 8 h. The chloride ions released from the membrane were titrated with a  $0.01 \text{ mol dm}^{-3}$   $\text{NaOH}$  aqueous solution. The IEC values were calculated from the released  $\text{H}^+$  ions and expressed as  $\text{mmol g}^{-1}$  of dry membrane (in the  $\text{Cl}^-$  form).

**Water Uptake.** Water uptake, a useful indicator for membrane swelling, was calculated according to the following equation

$$\text{WU\%} = 100 \times (W_1 - W_0) / W_0 \quad (2)$$

where  $W_0$  is the dry weight of the membrane and  $W_1$  is the wet weight of the membrane.

**Scanning Electron Microscopy (SEM).** Cross-section morphology of the blend membrane was examined by scanning electron microscopy. Dry membrane samples were manually fractured after cooling in liquid nitrogen. Specimens were sputter coated with palladium and imaged on a Hitachi S4500 scanning electron microscopy at  $10.0 \text{ kV}$ .

**Transmission Electron Microscope (TEM).** TEM study was carried out at  $200 \text{ K}$  on a JEM-2100 instrument. An amount of  $4 \mu\text{L}$  of  $1 \text{ wt \%}$  ( $100\% \text{HFSP}$ )-85 solution was dropped on to a carbon-coated copper grid, and the solvent (DMF) was then removed by heating at  $80^\circ\text{C}$  for 5 h under vacuum. A thin layer with an estimated thickness of  $50 \text{ nm}$  was obtained for TEM observations.

**Time-Resolved FTIR/ATR Analysis.** Time-resolved FTIR/ATR measurements<sup>14</sup> were performed at  $25^\circ\text{C}$  using Fourier transform infrared (FT-IR) analysis with a Jasco 460 plus spectrometer (Tokyo, Japan) equipped with a DTGS detector and a ZnSe IRE crystal. The membrane clipped between IRE crystal and filter papers was mounted in an ATR cell. As shown in the Figure 1, the ATR cell is equipped with a quadrature clamp, which can cover the crystal surface perfectly. We can control this clamp to ensure the tight contact between crystal and the membrane assembly and also to give a uniform pressure

distribution on the membrane during the measurement. The spectrum of the dry membrane was first collected as background. Then, without moving the sample, deionized water was injected into the top piece of filter paper when starting data collection. The spectra were recorded at a spectral resolution of  $1 \text{ cm}^{-1}$  by accumulating 10 scans. The measured wavenumber range was  $4000\text{--}400 \text{ cm}^{-1}$ .

**Proton Conductivity.** The proton conductivity of the FSP-SPPESK composite membrane was measured using the normal four-point probe technique.<sup>15</sup> An Autolab PGSTAT 30 (Eco Chemie, Netherland) was used to record the impedance data before conductivity calculation. The operation conditions were as follows: galvanostatic mode; ac current amplitude,  $0.1 \text{ mA}$ ; frequency, from  $1 \text{ MHz}$  to  $50 \text{ Hz}$ . The determined frequency region (phase angle  $\approx 0$ ) was about  $10000\text{--}500 \text{ Hz}$ . The proton conductivity ( $\kappa$ ) was calculated according to the following equation

$$\kappa = \frac{L}{RWd} \quad (3)$$

where  $R$  is the obtained membrane resistance;  $L$  is the distance between potential-sensing electrodes (here  $1 \text{ cm}$ ); and  $W$  and  $d$  are the width (here  $1 \text{ cm}$ ) and thickness of the membrane, respectively. During the measurements, the cell was placed inside a temperature and humidity controlled oven. In such a case, samples were exposed to humidified air, and their conductivities at different temperatures were determined by the impedance of fully hydrated samples.

**Evaluation of Performance in Fuel Cells.** The membrane electrode assembly (MEA) was prepared as follows: Pt/C electrode was prepared by spraying a catalyst, consisting of Pt/C catalyst (30 wt % Pt) and Nafion solution (Aldrich, 5 wt %, dissolved in ethanol), onto carbon cloth (E-TEK, USA). Then, the Pt/C electrode with a Pt loading of  $0.381 \text{ mg cm}^{-2}$  was put on the blend membrane, and the MEA was installed in the electrochemical cell chamber. All the fuel cell measurements were conducted in a flow of humidified  $\text{H}_2/\text{O}_2$  at  $0.1 \text{ MPa}$  ( $\text{H}_2 110 \text{ mL min}^{-1}$ , and  $\text{O}_2 110 \text{ mL min}^{-1}$ ) at  $60^\circ\text{C}$  under hydrous conditions.

## Results and Discussion

**Microstructure of Composite Membranes.** Figure 2 presents the microstructure of a FSP/SPPESK composite membrane (85 wt % FSP/15 wt % SPPESK), in which FSP has a protonation degree of 100%. This membrane is denoted as (100% HFSP)-85. In the scanning electron microscopy (SEM) image (Figure 2a), microspheres (SPPESK phase) scatter in the matrix (FSP phase). As further magnified by TEM, these microspheres have a core–shell structure (Figure 2b). In addition, there are some white spots in the microsphere region, which are attributed to high-intensity electronic beam (as high as  $200 \text{ K}$ ) during the TEM test. Obviously, the SPPESK phase is the core, but what is the “shell” composed of? To find the answer, a simple but interesting experiment can give some clues. During membrane preparation, when a  $\text{H}^+$ -form FSP–DMF solution and a  $\text{Na}^+$ -form SPPESK–DMF solution are mixed at  $25^\circ\text{C}$  (Figure 3c,d), a turbid suspension is obtained initially and divides into two layers afterward (Figure 3d). Surprisingly, when the mixture is heated at  $170^\circ\text{C}$  for 1 h, a miscible turbid suspension is obtained and will not delaminate again as it cools down (Figure 3e). According to the research of Eigen<sup>16,17</sup> and Weller,<sup>18</sup> general acid–base reactions in solutions are bimo-

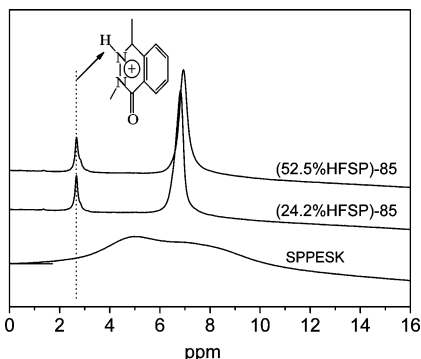


**Figure 4.** Solid state  $^1\text{H}$  NMR spectra of SPPESK, (24.2%HFSP)-85, and (52.5%HFSP)-85 membranes.

lecular in nature: diffusion of acid and base to form hydrogen-bonded encounter pairs, followed by intrinsic proton transfer within these encounter pairs.<sup>19</sup> Therefore, it is possible that the sulfonic acid groups in FSP and the phthalazone groups in SPPESK act as acid and base, respectively, to form hydrogen-bonded acid–base pairs via the available electron pair of  $-\text{N}=\text{}$  in SPPESK. This is responsible for the partial miscibility of the mixture at low temperature (Figure 3d). When temperature increases, the proton in the  $-\text{SO}_3\text{H}$  group has enough energy to transfer along the hydrogen bond to the base ( $-\text{N}=\text{}$  group), and the electrostatically interacted acid–base pairs are finally formed. In the solid state  $^1\text{H}$  NMR spectra (Figure 4), compared with the spectrum of  $\text{Na}^+$ -form SPPESK, a new peak at 2.3 ppm, which can be attributed to the  $\text{N}-\text{H}$  group, appears in the spectra of FSP/SPPESK composite membranes. This result conforms that hydrogen-bonded acid–base pairs are transformed to electrostatically interacted acid–base pairs when the proton in the acid transfers through the hydrogen bond to the base. Moreover, Figure 3c–e indicates that this intramolecular proton transfer is temperature dependent and irreversible. The possible chemical reactions are shown in Figure 3f. Hence, the “shell” must be composed of electrostatically interacted acid–base pairs. During solvent evaporation, a microphase separation occurs due to the transfer and aggregation of SPPESK and FSP molecules in each phase. As mentioned above, the acid–base interactions exist in the suspension, and the mobility of the acid–base complexes is much lower than those of free SPPESK or FSP molecules. Consequently, the acid–base complexes with a large number of “tentacles” (FSP polymer chains) twist and finally form a “shell”. During solvent evaporation, FSP molecules escape from the “shell” to the FSP-rich phase, while SPPESK molecules move and aggregate in the “shell”. Accordingly, the composite membrane has a multiphase morphology: SPPESK, encapsulated in a “shell”, is the core and scatters in a continuous phase (FSP). The “shell” is composed of electrostatically interacted acid–base pairs. The corresponding microstructure is proposed as Figure 2c.

**Local Fluctuation of Water Content in This Multiphase Membrane.** As stated in the Introduction, proton transfer depends largely on water content, so the hydration properties of these three phases were investigated by focusing on the relationship between the amount of acid–base pairs, water uptake, and IEC. During sample preparation, the SPPESK weight content was fixed at 15%, and the FSP protonation degree varied from 5.3% to 100%. As shown in Figure 5, significant reductions in both water uptake and IEC are observed in the membranes with FSP protonation degrees lower than 43.7%. The main cause is acid–base interactions. Generally speaking, water uptake and IEC depend mainly on the density

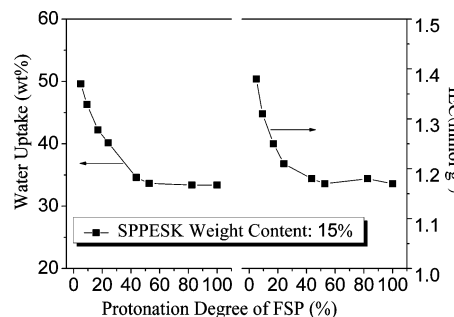


**Figure 5.** Effect of FSP protonation degree and SPPESK content on membrane water uptake and IEC.

of free sulfonic acid groups in the membrane. At a given SPPESK weight content, the total amount of sulfonic acid groups is constant. Therefore, as the FSP protonation degree increases, more sulfonic acid groups are converted into electrostatically interacted acid–base pairs, and the number of free sulfonic acid groups decreases. But when the FSP protonation degree is larger than 43.7%, neither water uptake nor IEC decreases further, indicating a saturation of acid–base pairs in the blend membrane at a given composition. On the other hand, the reductions in water uptake and IEC also imply that the sulfonic acid groups trapped in those interactions can not exchange ions, and the number of water molecules around the interacted sulfonic acid groups is much less than that around free sulfonic acid groups. Hence, the water content of the “shell” is much lower than that of the SPPESK or FSP phase.

**Proton Transfer in the Multiphase Membrane.** As stated above, there is a local fluctuation of water content in this multiphase membrane: two hydrophilic phase domains (SPPESK and FSP phases) are connected by a poorly hydrophilic phase (composed of acid–base pairs). As is well known, the proton affinity of water in forming hydronium ions ( $\text{H}_3\text{O}^+$ ) plays a significant role in proton transfer in hydrated proton-conducting membranes (the vehicle mechanism).<sup>20</sup> In this sense, the proton transfer in those two hydrophilic domains (SPPESK and FSP phases) must be in the vehicle mechanism. However, can these  $\text{H}_3\text{O}^+$  transfer through the poorly hydrophilic “shell” by the same mechanism? According to the results of IEC and water uptake measurement (Figure 5), the  $-\text{SO}_3\text{H}$  groups in these electrostatically interacted acid–base pairs can not adsorb as many water molecules as free  $-\text{SO}_3\text{H}$  groups. Moreover, the proton conductivity decreases with an increase in the protonation degree of FSP at a given temperature (Figure 6b). All the results indicate that protons can not transfer through the “shell” by the vehicle mechanism for lack of enough water molecules as vehicle. But surprisingly, membranes with different amounts of acid–base pairs exhibit similar fuel cell performance, i.e., similar efficiency of proton conduction under identical conditions (humidified  $\text{H}_2/\text{O}_2$  at 60 °C) (Figure 6a). Different from the principle of proton conductivity measurement, excess protons are generated from one electrode and transfer through the membrane during the fuel cell test. So the efficiency of proton conduction in these membranes is dependent not only on water content but also on effective proton transfer structures. Therefore, if there are some special proton-conducting structures in the “shell” to facilitate proton transfer other than  $\text{H}_3\text{O}^+$  transfer, the “shell” will not be a barrier for continuous proton transfer. Note that not all of the  $-\text{SO}_3\text{H}$  groups in the “shell” are trapped in the electrostatically interacted acid–base pairs, so those free  $-\text{SO}_3\text{H}$  groups must be involved in the proton-conducting structures. To probe into the information of  $-\text{SO}_3\text{H}$  in the proton-conducting structure, the time-resolved FTIR-ATR mea-

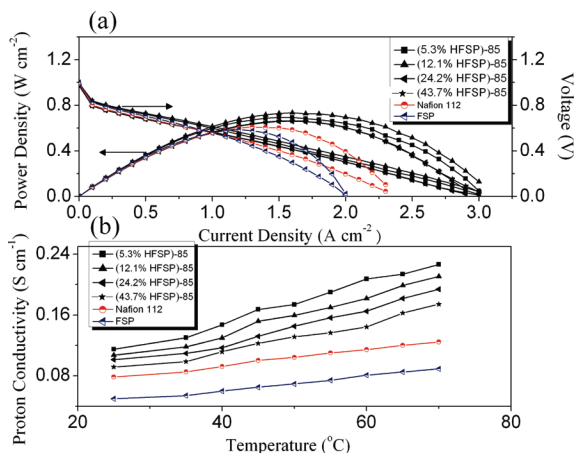


**Figure 6.** (a) Fuel cell performance of composite membranes. (b) Proton conductivities of membranes at increasing temperatures.

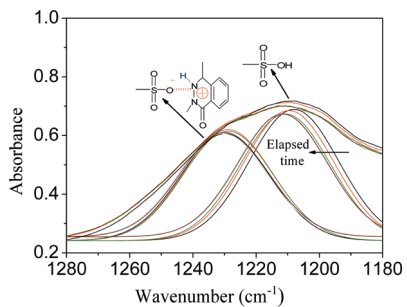


**Figure 7.** Time-resolved FTIR/ATR spectra of the (52.5%HFSP)-85 membrane during the diffusion of water into the membrane.

surement was performed during the diffusion of water into membrane. The FTIR spectra are presented in Figure 7 and have two broad bands overlapped in the range of 1260–1180 cm<sup>-1</sup>, which correspond to free sulfonic acid groups and the sulfonic acid groups under electrostatic interaction.<sup>21,22</sup> After water diffuses into the membrane, the absorption bands in this range

change slightly. The two overlapped bands are separated using the peak fitting module (PFM) of OriginPro 7.5, which offers the ability to automatically detect peak locations and provide highly accurate nonlinear least-squares curve fitting. The results are illustrated in Figure 7. While water is diffusing into the membrane, the band of O=S=O in the free sulfonic acid groups (centered at 1206 cm<sup>-1</sup>) decreases in intensity and shifts to higher frequency as a function of time, but the band of O=S=O in electrostatically interacted acid–base pairs (centered at about 1230 cm<sup>-1</sup>) has no change. Obviously, a new interaction (not electrostatic interaction) is established between acid and base in the shell under hydrous conditions. As reported about the reaction of acids and bases involving proton transfer in an aqueous solution, a loose (solvent-separated) complex is formed first, where acid and base are linked by an intermediate water bridge (the maximum number of water molecules between acid and base is three).<sup>23,24</sup> Therefore, it is possible that a string of hydrogen-bonded water molecules connects the free acidic and basic groups in the “shell” (Figure 8). Obviously, these loose acid–base pairs are responsible for the shift of the frequency in FTIR spectra. Note that the proton in the acid–base complex can transfer along the water bridge by the Grotthuss-type mechanism<sup>2,25</sup> until arrival at the base. For example, Bradley J. Siwick and Huib J. Bakker<sup>2</sup> find that the proton transfer between 8-hydroxy-1,3,6-pyrenetrisulfonic acid (HPTS) and acetate in aqueous solutions involves a water bridge connected with acid–base complexes. The proton is transferred inside these complexes via a Grotthuss-like mechanism through a hydrogen-bound chain of water molecules connecting HPTS and acetate. However, the proton can only transfer inside this complex from acid to base because there are no excess protons existing outside the complex. The situation is different in the hydrated proton-conducting membrane during the fuel cell test. Excess protons are generated from one electrode and usually combine with water molecules to transfer in hydrophilic domains of the membrane. When they arrive at the poorly hydrophilic interlayer, there are not enough water molecules as vehicles; hence, protons will find another channel for continuous transfer. Considering

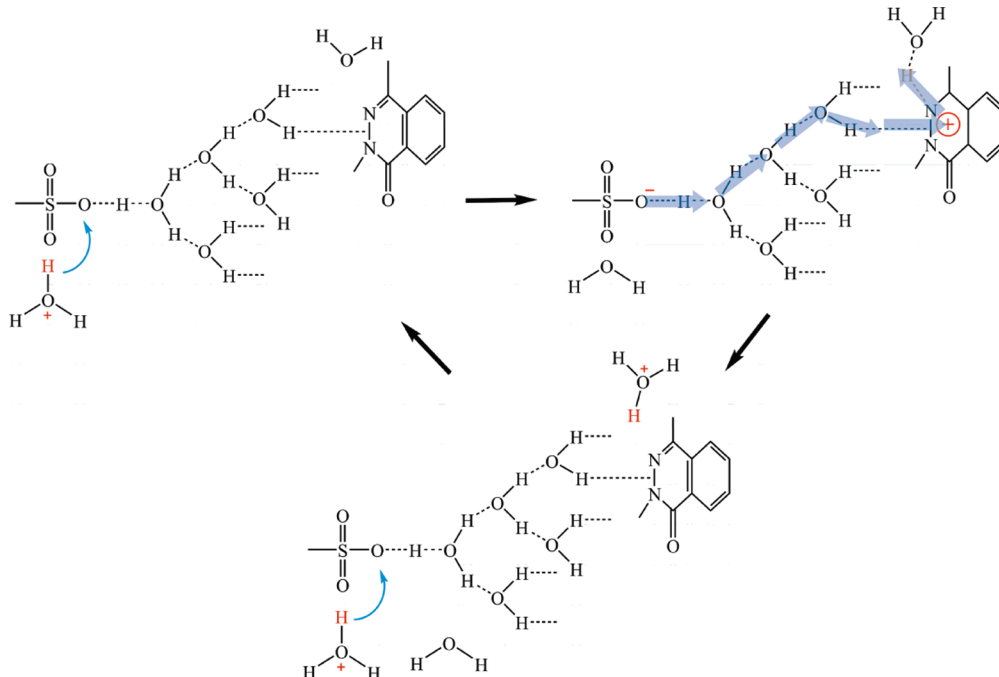


**Figure 8.** Schematic of the conduction model: proton transfer via a hydrogen-bonded (black dotted lines) acid–base pair. Blue arrows represent the direction of proton transfer.

protons, other than  $\text{H}_3\text{O}^+$ , can transfer within these hydrogen-bonded acid–base pairs,<sup>2,25</sup> we propose a novel proton-conducting channel for protons to transfer out of this “shell” (Figure 8) by hydrogen bonds breaking and forming. Particularly, the proton in  $\text{H}_3\text{O}^+$  first interacts with the  $-\text{SO}_3\text{H}$  group in this acid–base pair by hydrogen bonding, then transfers along the hydrogen bonds to arrive at the base, and finally moves out of the acid–base pair by hydrogen bonds forming and breaking between this proton and another water molecule. Accordingly, protons will transfer through the “shell” continuously in this manner. Do protons transfer through this poorly hydrophilic region via such a mechanism? Experiment results of water uptake and fuel cell performance can give some clues. According to the water uptake data in Figure 5, the amount of water molecules in this interlayer decreases with the number of electrostatically interacted acid–base pairs; i.e., vehicles for protons decrease in the same trends, and accordingly fuel cell performance would deteriorate. However, the fact as shown in Figure 6a is the opposite: fuel cell performance does not become worse even though water uptake decreases largely. The result indicates that protons can transfer in this poorly hydrophilic region through this unique structure other than combining with water molecules as in the vehicle mechanism. Because of this unique proton transfer mechanism, these composite membranes exhibit better electrochemical performances during fuel cell tests than those of pure FSP and commercialized Nafion-112 membranes: the maximum power density of the composite membrane reaches approximately  $990 \text{ mW cm}^{-2}$  at the current density of  $2600 \text{ mA cm}^{-2}$  and the cell voltage of 0.38 V (Figure 6a).

## Conclusions

The proton transport mechanism in hydrated multiphase material has been analyzed with emphasis on the role of water and hydrogen bonding structure. Experimental results show that the composite membrane possesses a multiphase microstructure: two highly hydrophilic regions (FSP and SPPESK) are connected by a poorly hydrophilic interlayer, which is composed of electrostatically interacted acid–base pairs. For application in fuel cells, excess protons transfer within SPPESK and FSP phases according to the vehicle mechanism; however, in the interlayer, proton-conducting channels constructed of hydrogen-bonded acid–base pairs facilitate proton transfer by hydrogen

bonds forming and breaking between acid–base pairs and water molecules. Because of the existence of the continuous proton transfer channel through the membrane, these composite membranes show higher fuel cell performance than Nafion-112 and pure FSP membrane in low temperature PEMFCs.

**Acknowledgment.** We thank the Natural Science Foundations of China, National Key Technology R&D Program of China (No.2006BAE02A01), the National Basic Research Program of China (No. 2009CB623403), the Joint Research Project under the KOSEF-NSFC Cooperative Program (No. 20911140273), and China Scholarship Council for financial support to this research.

## References and Notes

- (1) Hynes, J. T. *Nature* **1999**, *397*, 565.
- (2) Siwick, B. J.; Bakker, H. J. *J. Am. Chem. Soc.* **2007**, *129*, 13412.
- (3) Eigen, M. *Angew. Chem.* **1963**, *75*, 489.
- (4) Zundel, G.; Metzger, H. Z. *Naturforsch.* **1967**, *22a*, 1412.
- (5) Kreuer, K. D.; Rabenau, A.; Weppner, W. *Angew. Chem., Int. Ed. Engl.* **1982**, *21*, 208.
- (6) Agmon, N. *J. Chim. Phys. -Chim. Biol.* **1996**, *93*, 1714.
- (7) Spry, D. B.; Goun, A.; Glusac, K.; Moilanen, D. E.; Fayer, M. D. *J. Am. Chem. Soc.* **2007**, *129*, 8122.
- (8) Kreuer, K. D. *Solid State Ionics* **1997**, *97*, 1.
- (9) Paddison, S. J. *Annu. Rev. Mater. Res.* **2003**, *33*, 289.
- (10) Dippel, Th.; Kreuer, K. D. *Solid State Ionics* **1991**, *46*, 3.
- (11) Paddison, S. J.; Paul, R.; Kreuer, K. D. *Phys. Chem. Chem. Phys.* **2002**, *4*, 1151.
- (12) Gu, S.; He, G. H.; Wu, X. M.; Li, C. N.; Liu, H. J.; Lin, C.; Li, X. C. *J. Membr. Sci.* **2006**, *281*, 121.
- (13) Okada, T.; Moller-Holst, S.; Gorseth, O.; Kjelstrup, S. *J. Electroanal. Chem.* **1998**, *442*, 137.
- (14) Tang, B. B.; Wu, P. Y.; Siesler, H. W. *J. Phys. Chem. B* **2008**, *112*, 2880.
- (15) Sone, Y.; Ekdunge, P.; Simonsson, D. *J. Electrochem. Soc.* **1996**, *143*, 1254.
- (16) Eigen, M.; Kruse, W.; De, Maeyer, L. *Prog. React. Kinet.* **1964**, *2*, 285.
- (17) Eigen, M. *Angew. Chem., Int. Ed.* **1964**, *3*, 1.
- (18) Weller, A. *Prog. React. Kinet.* **1961**, *1*, 187.
- (19) Steiner, T. *Angew. Chem.* **2002**, *114*, 50.
- (20) Mohammed, O. F.; Pines, D.; Dreyer, J.; Pines, E.; Nibbering, E. T. *J. Science* **2005**, *310*, 83.
- (21) Deimede, V.; Voyatzis, G. A.; Kallitsis, J. K.; Qingfeng, L.; Bjerrum, N. *J. Macromolecules* **2000**, *33*, 7609.
- (22) Gieselmann, M. B.; Reynolds, J. R. *Macromolecules* **1992**, *25*, 4832.
- (23) Kreuer, K. D.; Paddison, S. J.; Spohr, E.; Schuster, M. *Chem. Rev.* **2004**, *104*, 4637.
- (24) Kreuer, K. D. *Chem. Mater.* **1996**, *8*, 610.
- (25) Mohammed, O. F.; Pines, D.; Dreyer, J.; Pines, E.; Nibbering, E. T. *J. Science* **2005**, *310*, 83.

JP905778T